chemosensors

Article

Principal Component Analysis of Transient Potential Signals from Ion-Selective Electrodes for the Identification and Quantification of Different Ions

José Antonio González-Franco [1], José Manuel Olmos [2,*], Alberto Ruiz [3] and Joaquín Ángel Ortuño [2,*]

[1] Department of Chemical Engineering, University of Murcia, 30100 Murcia, Spain; jagf@um.es
[2] Department of Analytical Chemistry, University of Murcia, 30100 Murcia, Spain
[3] Department of Informatics and Systems, University of Murcia, 30100 Murcia, Spain; aruiz@um.es
* Correspondence: josemanuel.olmos@um.es (J.M.O.); jortuno@um.es (J.Á.O.)

Abstract

This study investigates the potential of transient potentiometric signals generated by an array of ion-selective electrodes (ISEs) as the basis for a potentiometric electronic tongue capable of identifying and quantifying a range of inorganic and organic cations. Six distinct polymeric membrane ISEs were fabricated, differing in plasticizer type (either NPOE or DEHS), and in the presence or absence of a lipophilic ion exchanger (KTClPB) and/or an ionophore (DB18C6). Transient potential responses were recorded following the exposure of the electrode array to various cations at different concentrations. A total of 810 transient signals were analyzed through visual inspection and principal component analysis (PCA), revealing characteristic dynamic patterns influenced by membrane composition, ion type, and ion concentration. PCA was conducted both on the transient signals from each individual electrode and on the aggregated dataset comprising signals from the full six-electrode array (electronic tongue). The electronic tongue exhibited a markedly enhanced capacity for discriminating and quantifying ion concentrations in comparison to any single electrode.

Keywords: ion-selective electrode; potentiometry; transient potential signal; interfering ions; principal component analysis; electronic tongue

check for updates

Received: 25 June 2025
Revised: 5 August 2025
Accepted: 11 August 2025
Published: 13 August 2025

Citation: González-Franco, J.A.; Olmos, J.M.; Ruiz, A.; Ortuño, J.Á. Principal Component Analysis of Transient Potential Signals from Ion-Selective Electrodes for the Identification and Quantification of Different Ions. *Chemosensors* **2025**, *13*, 305. https://doi.org/10.3390/chemosensors13080305

Copyright: © 2025 by the authors. Licensee MDPI, Basel, Switzerland. This article is an open access article distributed under the terms and conditions of the Creative Commons Attribution (CC BY) license (https://creativecommons.org/licenses/by/4.0/).

1. Introduction

Under various designations, such as time-dependent phenomena [1], transient characteristics [2], transient phenomena [3], or transient signals [4], the dynamic behavior of ion-selective electrodes (ISEs) in the presence of interfering ions (i.e., ions other than the primary ion for which the electrode is designed) has been extensively reported in the literature. The presence of such interfering species induces a time-dependent evolution of the electrode potential, a behavior that has been observed across multiple ISE types, including glass electrodes [2,3], liquid membrane electrodes [1,4,5], precipitate-based ISEs [6], and plasticized polymeric membrane electrodes [4].

The transient potential signals of plasticized polymeric membrane ISEs incorporating a dissolved ion exchanger exhibit diverse signal profiles, depending on the nature of the interfering ion. [4,6–9]. For example, non-monotonic transient potential signals, characterized by an initial rapid potential overshoot followed by a slow relaxation, and slow monotonic transient potential signals, in which the potential increases constantly until reaching a stable value, have been reported [10].

A variety of theoretical models have been developed to describe, predict, and facilitate the interpretation of the dynamic response of ion-selective electrodes when exposed to interfering ions. The time-dependent nature of these signals arises from the interfacial ion exchange process between the primary ion present in the membrane and the interfering ion present in the sample, in conjunction with the mass transport of both species between the interface and the bulk of the phases. In this context, two main classes of models have been proposed: diffusion layer models, which consider diffusion as the sole mode of mass transport [8,11–16], and Nernst–Planck–Poisson models, which also account for ionic migration [17–20]. In both approaches, the simulated transient responses are influenced by thermodynamic parameters such as the partition coefficients of the primary and interfering ions between the aqueous sample phase and the membrane. Additionally, they depend on transport-related parameters, including the diffusion coefficients of both ions in each phase, the stirring rate of the aqueous phase, and the thickness of the diffusion layer. Furthermore, some models have incorporated electrokinetic parameters, such as ion transfer rate constants, to enhance their predictive accuracy [9].

The nature and concentration of the interfering ions can be determined by using electronic tongues, defined as a "multisensor system, which consists of a number of low selective sensors and uses advanced mathematical procedures for signal processing based on the pattern recognition (PARC) and/or multivariate analysis [artificial neural networks (ANNs), principal component analysis (PCA), etc."] [21,22]. The concept of electronic tongue (ET) was first introduced by Hayashi et al. [23], who developed a multi-channel potentiometric sensor for basic taste recognition. This system employed a network of membranes containing various lipids embedded in a plasticized PVC matrix. The sensor's responses to sour, sweet, bitter, salty, and umami flavors were evaluated using dilute hydrochloric acid, sucrose, quinine, sodium chloride, and monosodium glutamate, respectively. Since its initial application in taste identification, the electronic tongue concept has evolved to encompass systems capable of discriminating and classifying a wide range of liquid samples, enabling both qualitative and quantitative analyses [24].

A substantial number of electronic tongues have been developed, incorporating a wide range of transduction mechanisms, including potentiometric, amperometric, voltammetric, impedimetric, optical, piezoelectric, and hybrid modalities. These systems have been extensively reviewed in the literature [24–29]. Regardless of the transduction principle, it is essential that the individual components of the multisensor system exhibit differential responses to the various samples—a property referred to as cross-selectivity. In the case of voltammetric electronic tongues, such diversity can be achieved even with a single electrode, as each measurement generates a data matrix (current vs. potential) that captures the electrochemical fingerprint of the sample [30]. From this perspective, the IUPAC definition [21] may be viewed as limited. More broadly, the development of an electronic tongue requires only that a multivariate data matrix be obtained for each sample, enabling effective classification or quantification.

In potentiometric electronic tongues, the multisensor system typically comprises an array of generic (low-selectivity) ion-selective electrodes, although configurations combining both generic and highly selective electrodes have also been reported [31]. Most potentiometric electronic tongues rely on the measurement of equilibrium potentials at different electrodes. However, several studies have employed transient potential responses (i.e., potential as a function of time) recorded during the exposure of the electrodes to the sample. These dynamic responses can offer additional discriminatory information for sample differentiation [32,33], and in some cases, they have been utilized as the sole source of analytical information [7,34]. In this context, our research group has previously

demonstrated the feasibility of using the dynamic response of a single electrode for the multi-analyte determination of different ionic species [34].

The high complexity of the data generated by electronic tongue systems often necessitates the use of computational techniques for data analysis, pattern recognition, and machine learning, which have proven to be powerful tools in this context [24]. Although advanced methods for handling large-scale datasets have been developed, in our specific application domain—where the number of experimental samples is constrained by cost or practical limitations—it is more appropriate to employ simpler approaches, particularly visual inspection and linear modeling techniques [35].

In a previous study, transient potential signals were recorded for several inorganic and organic cations at different concentrations with a generic cation-selective polymeric membrane ISE and used for qualitative and quantitative purposes [7]. This paper extends that study by investigating the effects of plasticizer type on the membrane, as well as the presence of an ion exchanger and/or a generic ionophore, on transient signals for different monovalent, divalent, and trivalent cations, using six different electrodes. The signals obtained for different concentrations of each ion with the various constructed electrodes are applied to qualitative and quantitative analysis of the corresponding cations using Principal Component Analysis (PCA) and Principal Component Regression (PCR). The differential transient potential response of each membrane is exploited to build an electronic tongue, thereby improving the performance of the analysis.

2. Materials and Methods

2.1. Reagents and Solutions

Poly (vinyl chloride) (PVC) of high molecular weight, 2-nitrophenyl octyl ether (NPOE), bis-2-ethylhexyl-sebacate (DEHS), potassium tetrakis(4-chlorophenyl)borate (KTClPB, cation exchanger), dibenzo-18-crown-6 (DB18C6, ionophore) and tetrahydrofuran (THF) were of Selectophore grade from Sigma-Aldrich, Burlington, MA, USA. All other reagents used were of analytical reagent grade. Standard solutions of cations were prepared from their chloride salts (sodium Na^+, potassium K^+, ammonium $NH_4{}^+$, dopamine Dpm^+, copper Cu^{2+}, magnesium Mg^{2+}, calcium Ca^{2+} and procaine Prc^+), sulfate salts (copper Cu^{2+} and zinc Zn^{2+}), or nitrate salts (lanthanum La^{3+}), by dissolution in 18.2 MΩcm doubly deionized water (Milli-Q water systems, Merck Millipore, Germany). All the solutions were 1M, except for Prc^+ where concentration was 1×10^{-2} M. More diluted working solutions were prepared by diluting them with the same water.

2.2. Apparatus and Electrodes

A Selectophore Electrode Body ISE (Merck, Darmstadt, Germany) was employed in conjunction with a double-junction Ag/AgCl reference electrode (Orion 900200), containing a 1 M Li_2SO_4 solution in the outer compartment. Potentiometric measurements were carried out using a custom-built, high-impedance, six-channel millivoltmeter connected to a personal computer via USB, along with dedicated data acquisition software. Potential readings under zero-current conditions were recorded at 0.6s intervals to obtain potential versus time curves, with constant magnetic stirring maintained throughout the measurements.

2.3. Membranes Preparation

Six membranes were prepared by dissolving, approximately, 200 mg (66.3% w/w) of plasticizer (NPOE or DEHS) and 100 mg (33.2% w/w) of polymer (PVC) in 3 mL of THF. Additionally, the membrane cocktail contained 1.5 mg (0.5% w/w) of ion exchanger (KTClPB) and/or 2.2 mg (0.7% w/w) of ionophore (DB18C6). The exact composition of each membrane is presented in Table 1. The membrane solutions were poured into a Fluka

glass plate (inner diameter 28 mm, height 30 mm) and allowed to settle overnight until total evaporation of THF, thus obtaining thin plastic membranes. Then, 6 mm diameter pieces were cut out with a punch and incorporated into ISE bodies whose inner compartments were refilled with 1×10^{-3} M KCl as internal solution. The electrodes were conditioned by immersion in this same solution, also used to store the electrodes when not in use.

Table 1. Detailed composition of membranes and labels of ion selective electrodes (ISEs).

Components					
PVC	**Plasticizer**		**Ion Exchanger**	**Ionophore**	**ISE**
(wt.%)	**Compound**	**(wt.%)**	**KTClPB (wt.%)**	**DB18C6 (wt.%)**	
32.8	NPOE	66.7	0.5	0.0	1
33.2	NPOE	66.1	0.0	0.7	2
32.2	NPOE	66.6	0.5	0.7	3
33.1	DEHS	66.3	0.5	0.0	4
32.8	DEHS	66.5	0.0	0.7	5
32.9	DEHS	65.9	0.5	0.7	6

2.4. Measurement Procedure

Initially, the ion-selective electrodes (ISEs) and the reference electrode were immersed in 50 mL of a 1×10^{-6} M KCl solution, and the ISEs potentials were recorded under constant magnetic stirring at 700 rpm. After 20 s, a small volume (10–500 µL) of an appropriate working solution containing the target cation solution was added using a micropipette to achieve the desired concentration, without interrupting the potential measurement, which continued for an additional 50 s. Prior to each new measurement, the electrodes were rinsed with doubly deionized water and gently dried. All experiments were performed in triplicate.

2.5. Data Processing

The raw potentiometric transient signals were preprocessed by cutting off the portion of the signals corresponding to the first 18 s of the ion response. In addition, a baseline drift correction was performed. For each set of three signals corresponding to an ion concentration, the first potential value of the first signal was subtracted. Figure 1 shows the preprocessing of a typical set of raw signals.

The preprocessed transient signals were analyzed using Principal Component Analysis (PCA). Signals from each individual ISE were examined separately, as well as concatenated into a single feature vector combining the six ISE responses, allowing for joint analysis. PCA was employed to reduce the dimensionality of the dataset and to identify the principal modes of variation within the combined signals. The resulting low-dimensional representation was then correlated with sample composition using Principal Component Regression (PCR). PCR was selected due to the limited number of samples, as it helps mitigate overfitting by relying on a representation independent of the target variable. Multivariate linear calibrations were performed using PCR implemented with standard Python data analysis libraries (numpy 2.2.6, scikit-learn 1.6.1, matplotlib 3.10.3, and pandas 2.2.3) [35].

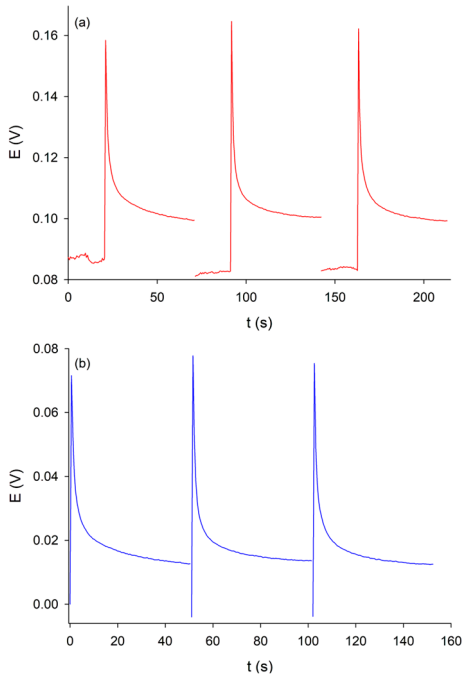


Figure 1. Typical set of three raw (**a**) and preprocessed (**b**) transient potential signals.

3. Results and Discussion

3.1. Influence of the Composition of the Membrane and the Ion Concentration on the Transient Potential Signals

The influence of the membrane composition on the transient potential signals of the six electrodes towards different cations was investigated. Specifically, the effects of the type of plasticizer, either NPOE (dielectric constant $\varepsilon = 21$) or DEHS ($\varepsilon = 4.2$) [36], and the presence of the cation exchanger KTClPB and the ionophore DB18C6, both individually and together, were examined. Six different electrodes were prepared: three containing the plasticizer NPOE (ISE1, ISE2, and ISE3) and three containing the plasticizer DEHS (ISE4, ISE5 and ISE6). The membranes of ISE1 and ISE4 incorporated only the cation exchanger, ISE2 and ISE5 contained solely the ionophore, and ISE3 and ISE6 included both the cation exchanger and the ionophore at a molar ratio of 2:1 (ionophore to cation exchanger) (see Table 1).

Transient potential signals were recorded for varying concentrations of monovalent cations (K^+, Dpm^+, Prc^+, NH_4^+, Na^+), divalent cations (Ca^{2+}, Mg^{2+}, Cu^{2+}, Zn^{2+}), and the trivalent cation La^{3+}, following the procedure described in Section 2.4. In general, concentrations of 1×10^{-6}, 1×10^{-5}, 1×10^{-4}, 1×10^{-3}, and 1×10^{-2} M were tested in triplicate. Exceptions included maximum tested concentrations of 1×10^{-3} M for Dpm^+, NH_4^+, La^{3+} and Zn^{2+}, and 1×10^{-4} M for Prc^+. Additionally, Cu^{2+} as sulfate was measured only at concentrations of 1×10^{-3} and 1×10^{-2} M. All transient signals obtained are provided in the Supporting Information (Figures S1–S11).

For illustrative purposes, the transient signals corresponding to the 1×10^{-3} M concentration of all cations studied are shown in Figure 2. To enhance clarity, the signals from each ISE have been offset horizontally in descending order according to their maximum transient potential value. In the case of procaine (Prc^+), signals at a lower concentration of 1×10^{-5} M are shown, as the electrodes exhibit significantly higher potential responses to this cation due to its pronounced lipophilicity.

As can be seen in Figure 2, the dynamic responses (potential versus time) recorded from the six electrodes generally show an initial rapid potential change, followed by a phase of gradual potential evolution until reaching a stable or near-stable final potential (E_f). Similar behavior was observed across other cation concentrations (see Supporting Information).

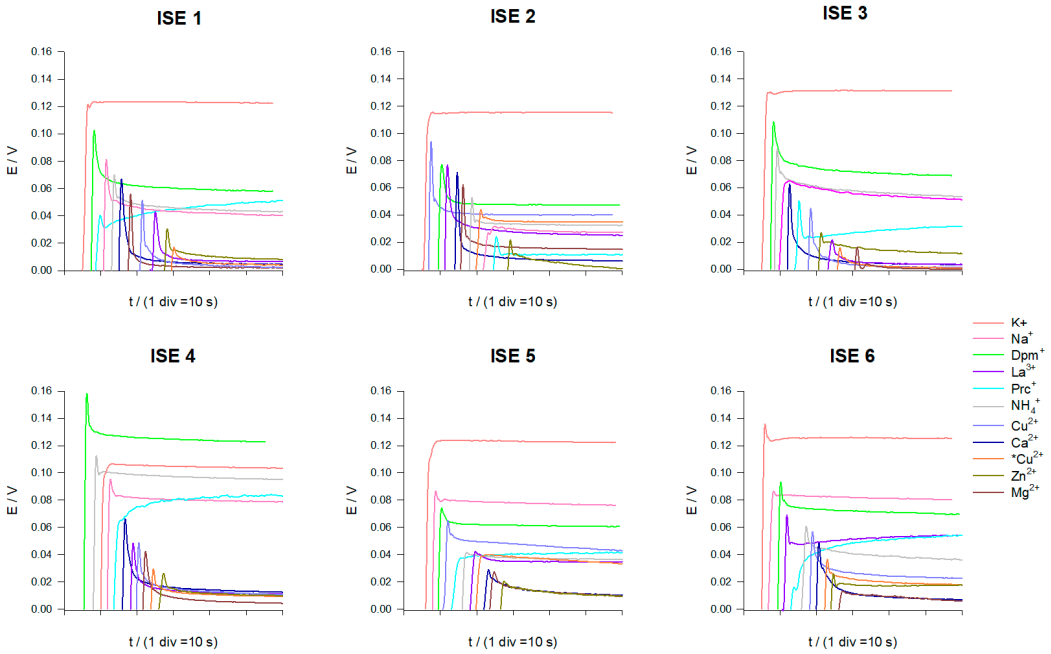


Figure 2. Transient potential signals for chloride solutions of K^+, Dpm^+, Prc^+, NH_4^+, Na^+, Ca^{2+}, Mg^{2+}, and Cu^{2+}; sulfate solutions of Zn^{2+} and Cu^{2+}; and nitrate solutions of La^{3+}. All the solutions are 1×10^{-3} M in KCl 10^{-6} M, except for Prc^+, the concentration of which is 1×10^{-5} M. * Cu^{2+}(sulfate).

Some authors have theoretically predicted the link between non-monotonic transient signals and physicochemical parameters. For example, Morf et al. [16] theoretically predicted a slow relaxation of the signal for interfering ions with selectivity coefficients much lower than 1, using E-t equations derived from a diffusion layer model. The relationship between selectivity coefficients and physicochemical parameters, such as partition coefficients and complexation constants, is well known [6]. Egorov et al. [8] developed an interface equilibria-triggered time-dependent diffusion model of the boundary potential that described experimental non-monotonic transient signals obtained using a picrate-selective electrode exposed to nitrate, an interfering ion with a low selectivity coefficient. Meanwhile, Hambly et al. [9] have predicted how ion exchange kinetics influence the corresponding non-monotonic transient signals in response to a step change in interfering ion concentration, by modeling the ion exchange between primary and interfering ions at the phase boundary.

For a systematic comparison of the signals obtained, both the final potential value (E_f) and the overall shape of the transient signals were considered. Electrodes with membranes containing only the lipophilic cation exchanger (ISEs 1 and 4) exhibited significant E_f values for all tested monovalent cations (potassium, dopamine, ammonium, sodium, and procaine—the latter measured at a 100-fold lower concentration), whereas E_f values for divalent (calcium, magnesium, copper, and zinc) and trivalent (lanthanum) cations were notably low. Furthermore, comparison of the E_f values for different monovalent cations between these two electrodes revealed distinct differences. For ISE1 (plasticized with NPOE), E_f was markedly higher for potassium relative to the other monocations. Conversely, for ISE4 (plasticized with DEHS), all E_f values for monovalent cations exceeded those observed with ISE1, except for potassium. In this case, the highest E_f value corresponded to dopamine, followed by potassium, ammonium, procaine, and sodium.

The E_f values observed for ISEs 1 and 4 can be interpreted by considering the differential solvation of the ions within the membrane, mediated by the respective plasticizer molecules. Notably, for potassium and ammonium—whose Gibbs free energies of hydration are reported to be very similar [37]—the E_f values obtained with ISE4 (plasticized with

DEHS) were also comparable, suggesting that the free energy of ion solvation within the membrane is similar for both cations. In contrast, with ISE1 (plasticized with NPOE), the E_f value for potassium was significantly higher than that for ammonium, indicating a more favorable solvation of potassium ions in this membrane composition.

Several studies in the literature have examined the influence of plasticizers on the equilibrium potentials and the corresponding selectivity coefficients of ion-selective electrodes. In this context, the work of Sakaki et al. [38] is particularly noteworthy. These authors investigated the effect of different plasticizers on the potentiometric response of electrodes incorporating a cation exchanger, both in the absence and presence of various ionophores, including several calix(n)arenes. A clear relationship was established between the selectivity profile of the electrodes and the dipole moment of the plasticizer used. Plasticizers with high dipole moments, such as 2-fluorophenyl-2′-nitrophenyl ether (FPNPE) and NPOE, yielded markedly different potential responses among various monovalent cations, following the order $Li^+ < Na^+ < NH_4^+ < K^+ < Rb^+ < Cs^+$. For instance, with FPNPE, the difference between the potential of 0.1 M Cs^+ and 0.1 M Li^+ was approximately 230 mV. In contrast, when using the low dipole moment plasticizer DEHS, the response order shifted significantly ($Cs^+ \approx Rb^+ \approx K^+ < Na^+ \approx NH_4^+ < Li^+$), and the potential difference between the highest and lowest responses—now between 0.1 M Li^+ and 0.1 M Cs^+—was reduced to about 140 mV. Based on these observations, and considering the affinity of FPNPE for "soft" cations such as Cs^+ and of DEHS for "hard" cations such as Li^+, the authors proposed that FPNPE acts as a "soft" plasticizer, while DEHS behaves as a "hard" plasticizer.

The higher response of K^+ in ISE1 compared to other inorganic cations is consistent with available information on the Gibbs energy values for ion transfer from water to NPOE or NPOE/PVC membranes. As can be seen in the bibliography, ion transfer is more favorable for K^+ than for Na^+ and NH_4^+ [39] and much more favorable than for Ca^{2+} [40]. In view of our results with ISE4, the same is expected with the plasticizer DEHS.

On the other hand, to the best of our knowledge, there are no previous studies in the bibliography on the influence of the plasticizer on the transient signal of ISEs towards different cations. As can be seen in Figure 2 for ISE1 and ISE4, a non-monotonic initial response—characterized by a potential overshoot—was observed for all foreign cations tested, with the exception of potassium, the primary ion initially present in the membrane. For monovalent cations, the potential overshoot constitutes only part of the overall transient signal, as the potential does not return to its baseline value prior to the concentration step. In contrast, for divalent and trivalent cations, the overshoot accounts for the majority—or entirety—of the signal, given that the potential typically returns to its initial value. Notably, ISE1 (plasticized with NPOE) exhibited greater potential overshoot than ISE4 (plasticized with DEHS), indicating that the plasticizer also influences the shape of the transient response. This finding is particularly relevant for the design of electronic tongues, where the ability to discriminate between analytes is enhanced by exploiting differences in transient signal profiles across a set of ion-selective electrodes.

Only low concentrations of procaine were employed, as its high lipophilicity results in markedly slow membrane regeneration following exposure to higher concentrations. In this case, the transient response obtained with the NPOE-plasticized membrane exhibited a slow potential increase following an initial non-monotonic overshoot. Conversely, the response with the DEHS-plasticized membrane also displayed a gradual potential increase, but without the initial overshoot.

The responses of the electrodes containing only the dibenzo-18-crown-6 (DB18C6) ionophore—ISE2 and ISE5—differed markedly from those of the corresponding electrodes containing only the cation exchanger (ISE1 and ISE4, respectively). Specifically, membranes incorporating DB18C6 exhibited significant final potential (E_f) values for divalent and

trivalent cations. This behavior can be attributed to the interaction between DB18C6 and the various ions, which significantly influence the potential response [41,42]. Notably, the E_f value for Cu^{2+} was particularly high, even surpassing that observed for the monovalent ammonium ion. A similarly elevated E_f value was found for trivalent lanthanum, in agreement with previous findings reported in [43], where a La^{3+}-selective electrode was constructed using dicyclohexane-18-crown-6 as ionophore in absence of a cation exchanger.

A comparison of the responses from electrodes ISE2 and ISE5 reveals that the membrane of ISE5—fabricated with the low dielectric constant plasticizer DEHS—exhibits a greater potential response to Na^+ than the corresponding membrane containing NPOE (ISE2). This observation is consistent with the findings reported by Sakaki et al. for other ionophores [38]. Moreover, as previously noted for the membranes containing only the cation exchanger (ISE1 and ISE4), the DEHS-based membrane containing only the ionophore (ISE5) produced less pronounced non-monotonic transient signals than its NPOE-based counterpart (ISE2), indicating that the plasticizer also modulates the dynamic response profile in ionophore-only systems.

In the case of electrodes ISE3 and ISE6, which incorporate both the cation exchanger and the ionophore, it is noteworthy that the response profile of ISE3—constructed with the NPOE plasticizer—closely resembles that of ISE1, which contains only the cation exchanger in the same plasticizer matrix. Conversely, the response profile of ISE6—plasticized with DEHS—is highly similar to that of ISE5, which includes only the ionophore in a DEHS-based membrane. These observations suggest that, in membranes containing both components, the influence of the cation exchanger dominates in the presence of NPOE, while the ionophore exerts a more pronounced effect in DEHS-based membranes.

The good response to K^+ with all the electrodes containing the ionophore DB18C6 (ISE2, ISE3, ISE5 and ISE6) can be explained, besides the abovementioned for ISE1 and ISE4, by the high complexation constants between this cation and 18C6 ether derivatives [44].

Ion concentration also influences both the shape of the transient signals and the magnitude of the final potential (E_f). In all cases, increasing the ion concentration resulted in a corresponding increase in the transient membrane potential. However, the E_f value for certain ions was found to be concentration-dependent only for specific electrodes. As illustrative examples, the transient responses obtained for varying concentrations of Cu^{2+} (as chloride) and K^+ are presented in Figures 3 and 4, respectively.

In the case of Cu^{2+} (Figure 3), the highest final potential (E_f) values were observed for electrodes ISE2 and ISE5, which contain only the ionophore. For ISE2, the differences in E_f across successive concentration decades remained relatively constant over the 1×10^{-2} to 1×10^{-5} M range, indicating a broader linear dynamic range compared to ISE5. Although both electrodes exhibited non-monotonic responses at all concentrations, ISE2 showed a more pronounced degree of non-monotonicity. In contrast, for the remaining electrodes (ISE1, ISE3, ISE4, and ISE6), the effect of Cu^{2+} concentration on the potential response was minimal—particularly for those with NPOE-based membranes (ISE1 and ISE3). These findings underscore the critical role of the ionophore in facilitating the detection of Cu^{2+}.

On the other hand, the six electrodes respond very well and nearly identical to the primary ion K^+ (Figure 4). In this case, the E_f value was clearly dependent on ion concentration and was reached rapidly, without any overshoot, across all ISEs. Notably, Figure 4 includes the three replicate measurements recorded for each concentration and electrode, demonstrating the high repeatability of the response to K^+. This behavior is attributed to the fact that K^+ is the primary ion present in the membranes; thus, its presence does not induce significant ion exchange and alteration of the membrane composition, resulting in stable and reproducible responses.

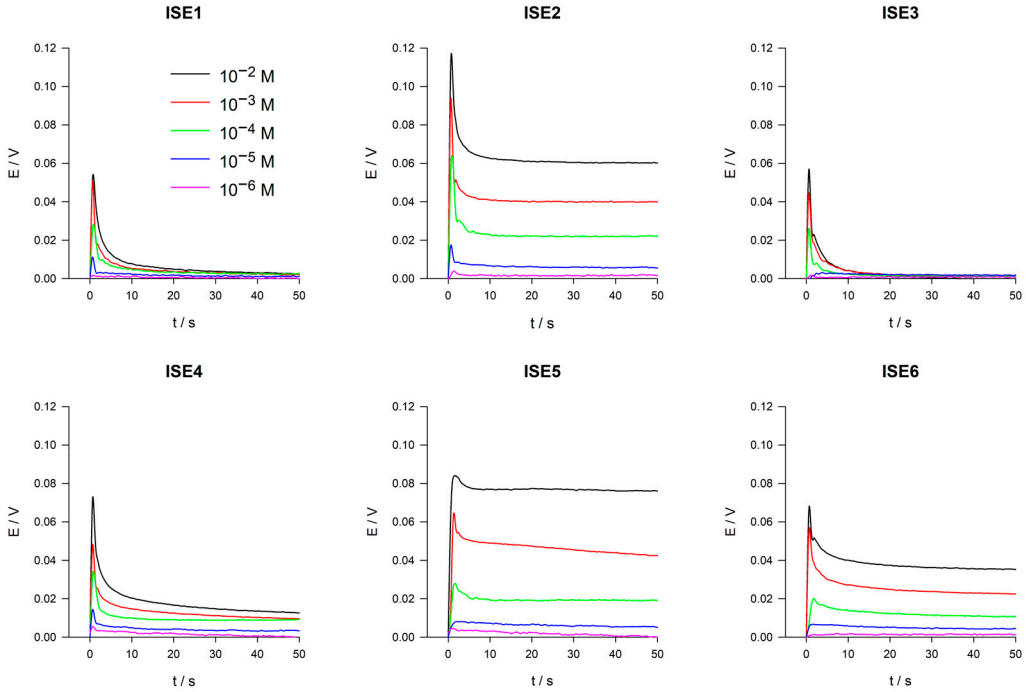


Figure 3. Transient potential signals from the six electrodes at different Cu^{2+} (as chloride) concentrations.

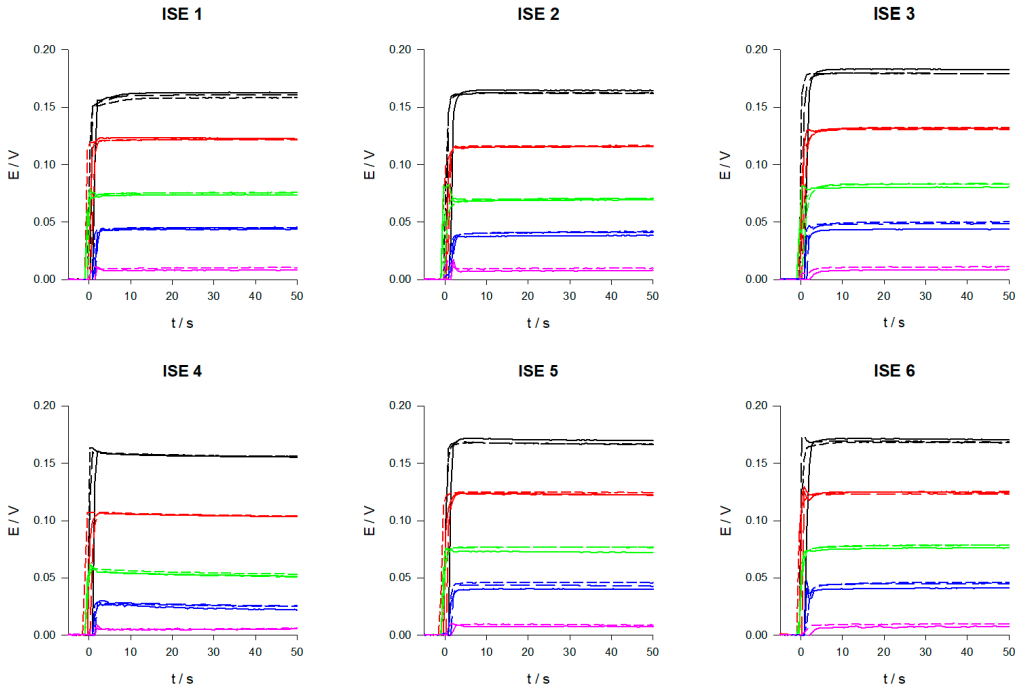


Figure 4. Transient potential signals from the six electrodes at different K^+ concentrations (in triplicate). The colors used for each concentration are identical to those in Figure 3. The different lines for each concentration represent the three replicate measurements.

In order to check the stability of the transient potential responses of the six ISEs, the signals corresponding to Na^+ at 10^{-3} M were recorded at different days as control. The results are shown in the Supporting Information (Figure S12). The signals are reasonable constants during a week, with only a slight variation in their magnitude.

The influence of ion concentration on the responses of other cations can be observed in the Supporting Information (Figures S1–S11). Although each ion exhibits distinct behavior, some general trends can be identified. For instance, the effect of ion concentration on the E_f

values for Mg^{2+} and NH_4^+ follows patterns similar to those observed for Cu^{2+} (as chloride) and K^+, respectively.

3.2. Principal Component Analysis of the Transient Potential Signals

3.2.1. Individual Principal Component Analysis for Each ISE

First, individual Principal Component Analysis was performed for the transient signals obtained with each ISE at the different ions and concentrations assayed. The original potential-time data, after preprocessing as indicated in Section 2.5, were projected onto a new basis consisting of a small number of signals (the principal components, PCs). In this way, the transient potential signal of an ion at a determined concentration for each ISE can be expressed as the sum of the average signal for that ISE and a linear combination of the PCs, with the contributions of the PCs being called PC-scores. The impact of each PC on the signal is lower as the order of the PC increases.

In our study, as shown in Figure 5, two PC scores are enough to explain the majority of the signal variance ($\geq$99.4%). This figure presents the principal component maps (PC maps) for the first two PCs of each ISE, plotting the PC2 score against the PC1 score. Although certain ions at specific concentrations are clearly separated from others, this is not the case for all ions and concentrations. This is due to the large variety of ions and concentration levels in the dataset. Reducing this diversity could potentially enhance discrimination. Nevertheless, a general trend is observed as follows: higher ion concentrations correspond to greater separation distances on the PC maps.

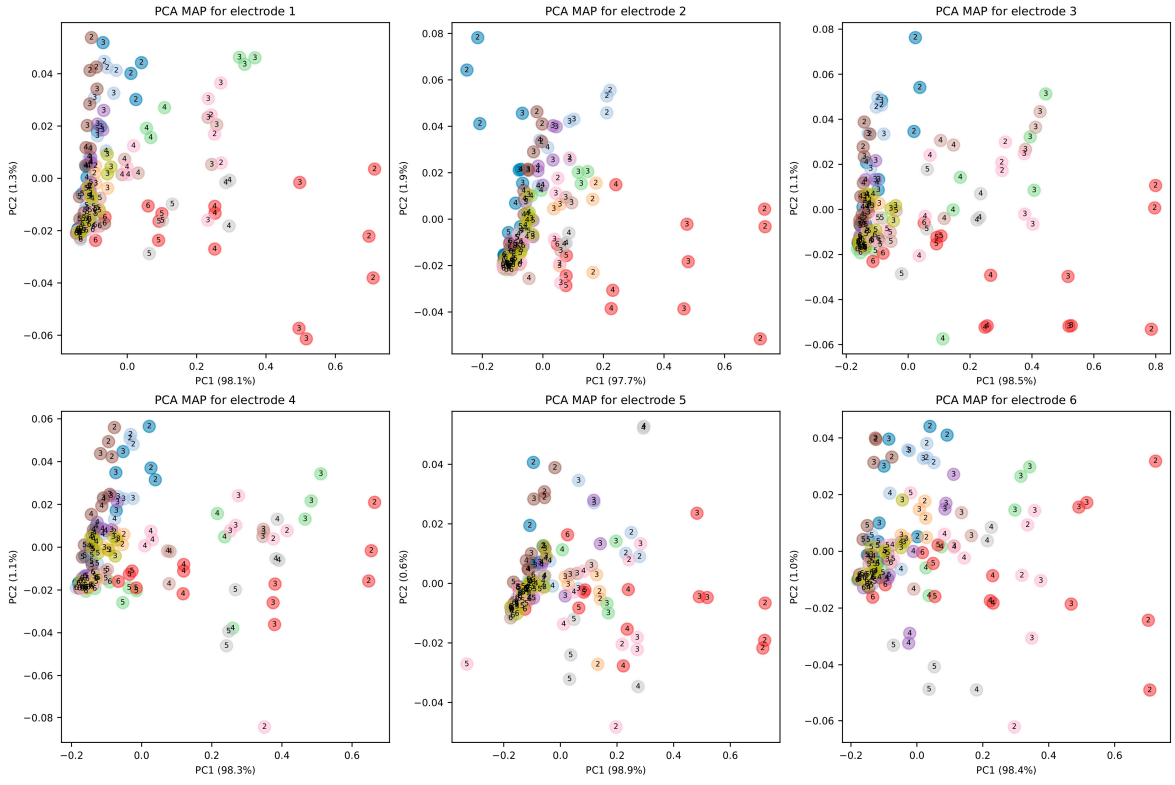


Figure 5. PC2 vs. PC1 maps obtained for each ion-selective electrode. The numbers in each circle correspond to the negative exponent of the concentration expressed in scientific notation (for example, the number 3 indicates a concentration of 10^{-3} M). The color of the circle represents the ion analyzed (see Figure 6 for the color legend). Note that the points corresponding to the three repetitions performed with each ion and concentration are plotted.

The results for each ion differ in each PC-map in Figure 5, reflecting the distinct transient potential responses that each ISE exhibits toward the different ions (see Figure 2).

Moreover, integrating the signals from all these ISEs offers a promising strategy for creating an electronic tongue, as will be illustrated in the next section.

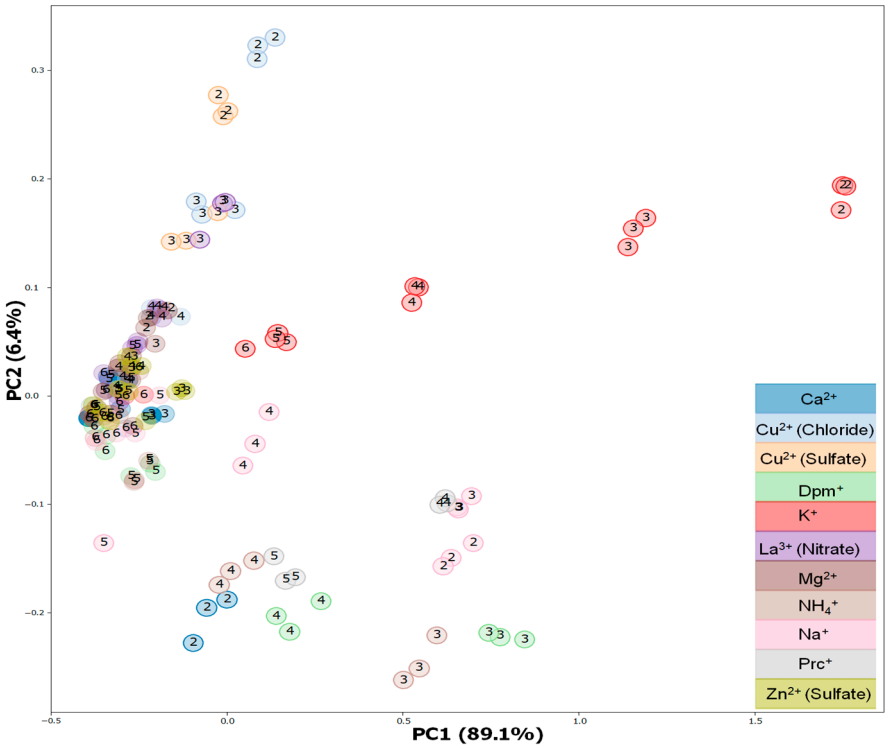


Figure 6. PC2 vs. PC1 map for the whole pool of transient signals obtained with the six ion-selective electrodes (electronic tongue). Unless indicated otherwise, the cations are in the form of chloride salt. See Figure 5 for the number interpretation.

3.2.2. Principal Component Analysis for a Multi-Electrode System of All ISEs (Electronic Tongue)

PCA was also performed on the complete set of transient signals (810 signals) collected from the six electrodes across all ions and tested concentrations. Figure 6 shows the principal component map based on the first two PCs (PC2 versus PC1), which together explain 95.1% of the total variance. This combined analysis significantly improves the individual electrode maps, simplifying data interpretation (see Figures 5 and 6). For example, the data points representing the primary ion (K^+) are now clearly separated from those of interfering ions and are aligned according to increasing concentration. Additionally, Cu^{2+}—whether as chloride or sulfate—shows good separation at higher concentrations and exhibits nearly identical slopes in the plot (Figure 6).

We also explored maps combining other principal component scores. Figure 7 display the plots of PC3 versus PC1 and PC3 versus PC2. These maps provide additional information to that offered by the first two principal components (Figure 6). For example, NH_4^+ ions are more distinctly separated from other ions in these plots. Notably, this clearer distinction appears in both maps, even though the combined variance explained by PC3 and PC2 is only about 8% (Figure 7 right). The usefulness of high-order PCs has also been recognized by other authors, for example, in differentiating food samples such as yogurts, wines, coffees and juices [45–47].

3.2.3. Application of the Transient Signals to Quantitative Analysis

Principal Component Analysis of the transient potential signals can also be applied for quantitative purposes [7,34]. The scores of the first two principal components (PC1 and PC2), obtained individually for each ion-selective electrode (ISE) and for the electronic

tongue (consisting of all six ISEs), were fitted using Principal Component Regression (PCR) to the following equation:

$$\log C = a\ PC1 + b\ PC2 + c \quad (1)$$

where C is the concentration of the ion, and a, b, and c are constants specific to each ion. Using individual electrodes, two principal components (PCs) explain over 99.4% of the variance. However, with the electronic tongue, this explained variance decreases to 95.1%. Therefore, for the electronic tongue, a similar equation incorporating six principal components was also used.

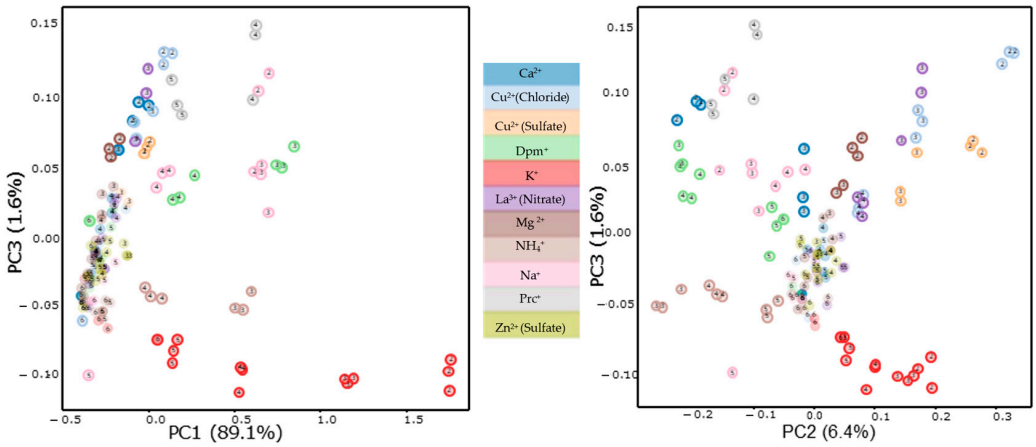


Figure 7. PC3 Vs. PC1 (**left**) and PC3 Vs. PC2 (**right**) maps for the whole pool of transient signals obtained with the six ion-selective electrodes (electronic tongue). See Figure 5 for the number interpretation.

Figure 8 shows the determination coefficients (R^2) found for each ion. As can be seen, individual ISEs are generally suitable for quantitative analysis. However, the combination of all six ISEs into an electronic tongue enhances the results ($R^2 \geq 0.92$). A paired *t*-test comparing the R^2 values of individual electrodes and the electronic tongue showed a significant improvement in ion quantification for the electronic tongue compared to electrodes ISE3, ISE5, and ISE6 (p-value < 0.02). This advantage becomes even clearer when six principal components are used, with R^2 values approaching unity for most ions (except for Ca^{2+}, which has an R^2 of 0.96). Moreover, the *t*-test confirmed that these improvements were statistically significant compared to any single electrode (p-value < 0.06).

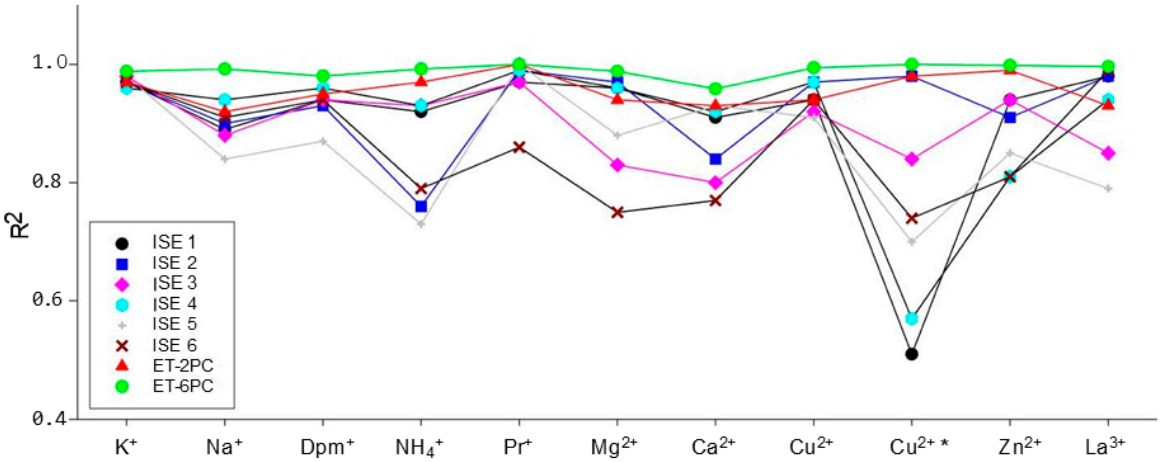


Figure 8. Individual ISEs (2PC) Vs. electronic tongue ET (2PC and 6PC). * Cu^{2+}(sulfate).

To illustrate the effectiveness of Equation (1) for quantifying ion concentration, Figure 9 left displays three-dimensional plots of the electronic tongue's PC1 and PC2 scores against

the logarithm of concentration (log C) for selected ions (Na^+, Zn^{2+}, La^{3+}, and Dpm^+). These plots also include the plane described by the equation. Similar plots for the other ions are provided in Figures S13–S19. As can be seen, the experimental data points at each concentration of each ion lie on or very near the plane.

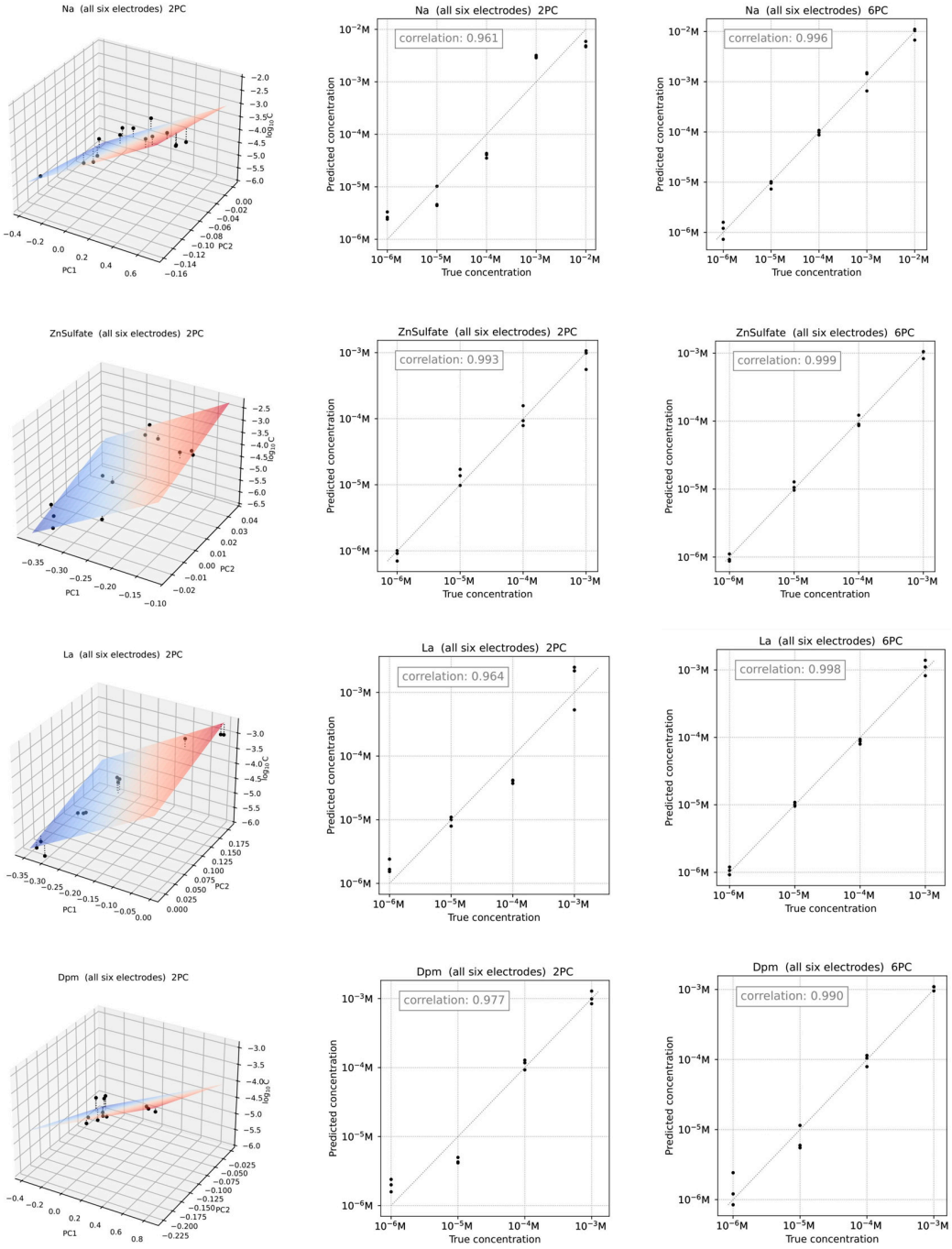


Figure 9. Plots 3D of the PC1 and PC2 scores versus log C (**left**) and plots of the concentration values predicted with two (**center**) and six (**right**) PCs versus the true values of the electronic tongue (six electrodes) for some ions.

The quantitative performance of the chemometric model is further validated in Figure 9 center, where the concentrations predicted by Equation (1) are plotted against the true concentrations. The points lie very close to the ideal line with a slope of one, as reflected by the correlation coefficients shown in the figure. The agreement between predicted and actual concentrations is nearly perfect when using six principal components, as illustrated

in Figure 9 right. It is worth noting that the improvement gained by employing more PCs is especially noticeable for Na^+ and La^{3+}.

3.2.4. Reconstruction of the Transient Signals of the Electronic Tongue from PCA

Each experimental transient signal collected with the electronic tongue for every ion and concentration consisted of 498 potential-versus-time data points (83 data points per electrode × 6 ISEs). As previously shown, applying PCA significantly reduces this high dimensionality. Additionally, the multivariate analysis allows the original transient signals to be reconstructed from the principal component scores [7]. This capability helps to confirm the effectiveness of the chemometric model used for ion identification and quantification. Another advantage of reconstructing the signals is the reduction or elimination of experimental noise, which otherwise complicates data analysis [48,49].

During the PCA reconstruction process, the original raw signals are reproduced using the minimum number of principal components necessary to achieve an accurate result. Figure 10 presents the reconstructed transient signal for Cu^{2+} (in the form of chloride) at 10^{-2} M obtained from the electronic tongue using four and nine principal components (i.e., four- and nine-dimensional score vectors). As shown, 4 PCs are only capable of partially reproducing the signal, while the use of 9 PCs results in excellent agreement between the original and reconstructed signals. Reconstructions of other electronic tongue signals can be found in the Supporting Information (Figures S20 and S21).

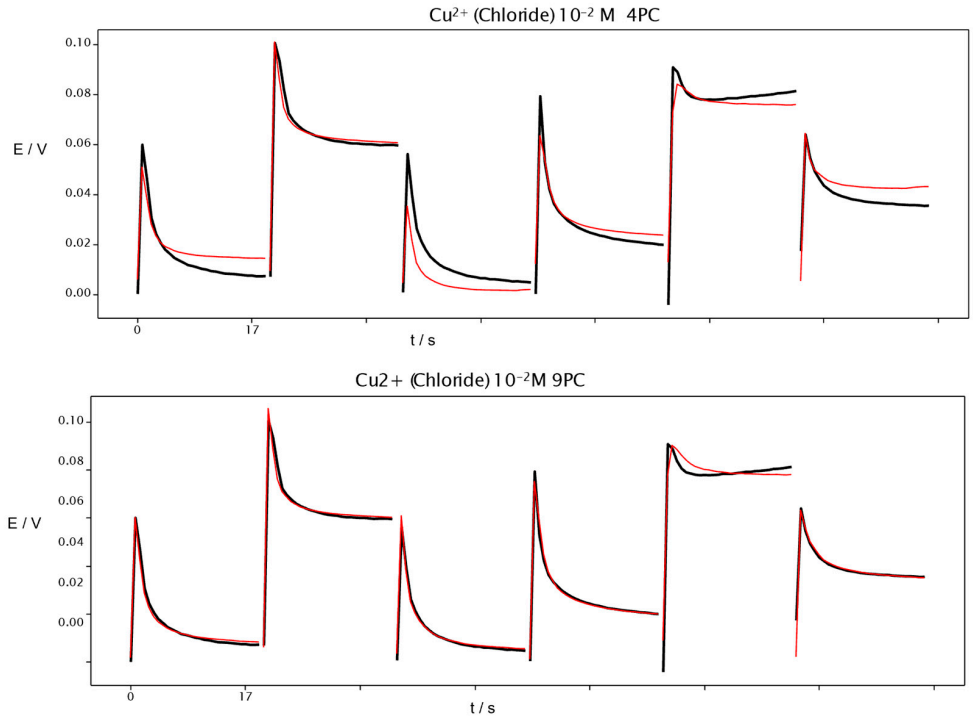


Figure 10. Reconstructions of the concatenated signals of the six ISEs (electronic tongue) of Cu^{2+} (as chloride) at 10^{-2} M using four and nine principal components.

Figure 11 displays the shape of the nine principal components used to reconstruct the Cu^{2+} signal described above. The mean signal obtained from the entire dataset—comprising all ions and concentrations—is also included as a solid line in each graph. This is because the shape of the principal components alone does not fully capture the variability they represent; instead, they contribute to the reconstructed signal by being added to the mean signal in specific proportions, either positive or negative. In Figure 11, each principal

component is shown added to the mean signal at ±10% (dotted lines). These resulting curves illustrate the extent of variation in the E–t signal along each principal direction.

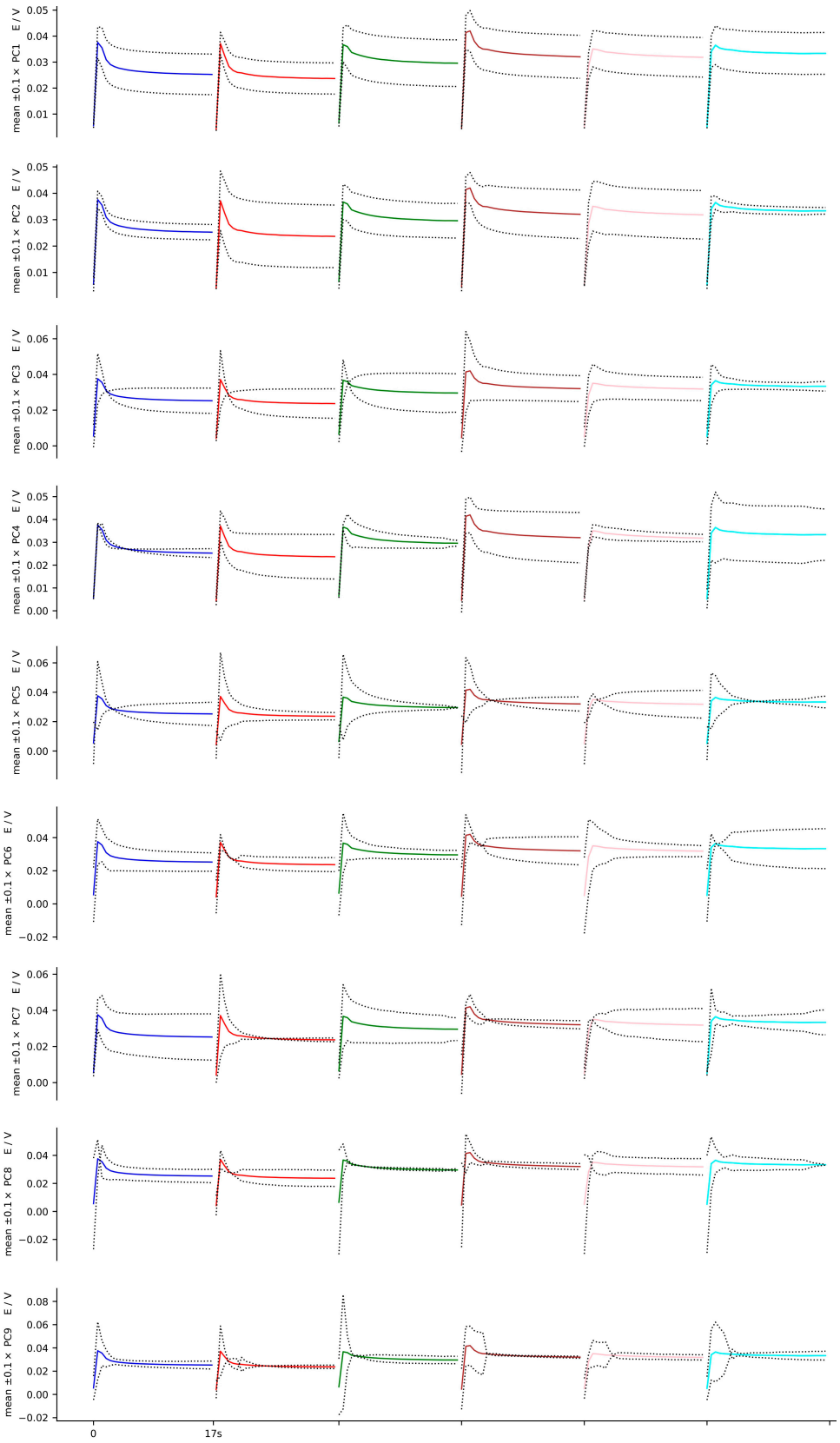


Figure 11. Mean signal obtained with the electronic tongue (solid lines) and curves resulting after adding the 9 principal component at ±10% (dotted lines). Different colors are used for the different ISEs of the electronic tongue.

4. Conclusions

This paper demonstrates the high impact of membrane composition (type of plasticizer (NPOE or DEHS) and the presence of a cation exchanger (KTClPB) and/or a low-selectivity profile ionophore (DB18C6)) on the transient potential signals toward different cations. The type of membrane influences both the signal shape and the final stationary potential value (E_f). Additionally, the key role of membrane composition is confirmed when analyzing the effect of varying ion concentrations. Thus, while the transient membrane response always increases with concentration, the E_f value for certain ions depends on the concentration only for certain membranes.

Principal Component Analysis (PCA) reduced the dimensionality of the experimental data, enabling qualitative and quantitative analysis. PC maps and Principal Component Regression (PCR) were produced using the transient signals obtained from each individual ISE. These were able to discriminate between some ions and predict their concentrations based on the PC scores. Furthermore, combining the signals of the 6 ISEs to form an electronic tongue offered more accurate results. The chemometric model with the electronic tongue was also useful for reconstructing the transient signals from the PCA results, showing excellent agreement with the original signals when 9 PCs were used.

We reckon that the approach adopted in this paper could be applied to other plasticizer/ionophore combinations and ion populations. However, further studies are needed to assess the usefulness of the present approach for analyzing real samples, to investigate the stability of transient signals in depth under different conditions and to study the robustness of the proposed platform. Also, extending the PCA treatment of transient potential responses to mixtures of ions would be useful to establish real possibilities of application.

Supplementary Materials: The following supporting information can be downloaded at: https://www.mdpi.com/article/10.3390/chemosensors13080305/s1, Figures S1–S11: Preprocessed set of transient potential signals obtained for all cations tested at different concentrations with the different ISEs. Figure S12: Preprocessed transient potential signals for 10^{-3} M Na^+ with the six ISEs over the course of a week. Figures S13–S19: 3D plots of the PC1 and PC2 scores versus log C (left) and plots of the concentration values predicted with two (center) and six (right) PCs versus the true values of the electronic tongue (six electrodes) for K^+, NH_4^+, Prc^+, Ca^{2+}, Mg^{2+}, and Cu^{2+} (as chloride and sulfate). Figures S20 and S21: Reconstructions of the concatenated potential transient signals of the six ISEs (electronic tongue) of Ca^{2+} and Cu^{2+} (as sulfate) at 10^{-2} M using four and nine principal components.

Author Contributions: Conceptualization, J.Á.O. and J.M.O.; methodology, J.Á.O., J.M.O., J.A.G.-F. and A.R.; software, A.R.; validation, J.Á.O., J.M.O., J.A.G.-F. and A.R.; formal analysis, J.A.G.-F. and A.R.; investigation, J.A.G.-F.; writing, J.Á.O., J.M.O., J.A.G.-F. and A.R. All authors have read and agreed to the published version of the manuscript.

Funding: This research was funded by the Ministerio de Ciencia e Innovación, Spain, grant number PID2022-136568NB-I00.

Institutional Review Board Statement: Not applicable.

Informed Consent Statement: Not applicable.

Data Availability Statement: The original contributions presented in this study are included in the article. Further inquiries can be directed to the corresponding author(s).

Conflicts of Interest: The authors declare no conflicts of interest.

References

1. Mathis, D.E.; Stover, F.S.; Buck, R.P. Ion Transport in Free and Supported Nitrobenzene Aliquat Nitrate Liquid Membrane Ion-Selective Electrodes. *J. Memb. Sci.* **1978**, *4*, 395–413. [CrossRef]
2. Karlberg, B. The Transient Characteristics of the Two-Ion Response of Hydrogen Selective Glass Electrodes. *J. Electroanal. Chem. Interfacial Electrochem.* **1973**, *42*, 115–126. [CrossRef]
3. Rechnitz, G.A.; Kugler, G.C. Transient Phenomena at Glass Electrodes. *Anal. Chem.* **1967**, *39*, 1682–1688. [CrossRef]
4. Ortuño, J.A.; Sánchez-Pedreño, C.; de Bobadilla, R.F. Transient Signals with an Antimony(V) Ion-Selective Electrode: The Relative Signal Return Rate as a Selectivity Parameter. *Talanta* **1994**, *41*, 627–630. [CrossRef]
5. Bagg, J.; Vinen, R. Response of a Calcium-Selective Electrode in Acid Solutions. *Anal. Chem.* **1972**, *44*, 1773–1777. [CrossRef]
6. Mikhelson, K.N. *Ion-Selective Electrodes*; Lecture Notes in Chemistry; Springer: Berlin/Heidelberg, Germany, 2013; Volume 81, ISBN 978-3-642-36885-1.
7. González-Franco, J.A.; Ruiz, A.; Ortuño, J.A. Dynamic Potentiometry with an Ion-Selective Electrode: A Tool for Qualitative and Quantitative Analysis of Inorganic and Organic Cations. *Chemosensors* **2022**, *10*, 116. [CrossRef]
8. Egorov, V.V.; Novakovskii, A.D.; Zdrachek, E.A. An Interface Equilibria-Triggered Time-Dependent Diffusion Model of the Boundary Potential and Its Application for the Numerical Simulation of the Ion-Selective Electrode Response in Real Systems. *Anal. Chem.* **2018**, *90*, 1309–1316. [CrossRef] [PubMed]
9. Hambly, B.; Guzinski, M.; Pendley, B.; Lindner, E. Kinetic Description of the Membrane-Solution Interface for Ion-Selective Electrodes. *ACS Sens.* **2020**, *5*, 2146–2154. [CrossRef]
10. Ortuño, J.A.; Sánchez-Pedreño, C.; Martinez, D. Nonmonotonic Transient Potential Signals with an 18-Crown-6 Based Ion-Selective Electrode in a Flow-Injection System. *Electroanalysis* **2003**, *15*, 1536–1540. [CrossRef]
11. Morf, W.E.; Lindner, E.; Simon, W. Theoretical Treatment of the Dynamic Response of Ion-Selective Membrane Electrodes. *Anal. Chem.* **1975**, *47*, 1596–1601. [CrossRef]
12. Egorov, V.V.; Novakovskii, A.D. Application of the Interface Equilibria-Triggered Dynamic Diffusion Model of the Boundary Potential for the Numerical Simulation of Neutral Carrier-Based Ion-Selective Electrodes Response. *Anal. Chim. Acta* **2018**, *1043*, 20–27. [CrossRef]
13. Egorov, V.V.; Novakovskii, A.D.; Zdrachek, E.A. Modeling of the Effect of Diffusion Processes on the Response of Ion-Selective Electrodes by the Finite Difference Technique: Comparison of Theory with Experiment and Critical Evaluation. *J. Anal. Chem.* **2017**, *72*, 793–802. [CrossRef]
14. Bakker, E.; Bühlmann, P.; Pretsch, E. The Phase-Boundary Potential Model. *Talanta* **2004**, *63*, 3–20. [CrossRef] [PubMed]
15. Olmos, J.M.; González-Franco, J.A.; Molina, A.; Ortuño, J.Á.; Laborda, E. OFF–ON Stirring Potentiometry with Solvent Polymeric Membrane Ion-Selective Electrodes: A Theory-Guided Approach to Foreign Ions. *J. Electroanal. Chem.* **2025**, *977*, 118828. [CrossRef]
16. Morf, W.E.; Pretsch, E.; de Rooij, N.F. Theory and computer simulation of the time-dependent selectivity behavior of polymeric membrane ion-selective electrodes. *J. Electroanal. Chem.* **2008**, *614*, 15–23. [CrossRef] [PubMed]
17. Lingenfelter, P.; Sokalski, T.; Lewenstam, A. Numerical Solution of the Coupled Nernst-Planck and Poisson Equations for Ion-Selective Membrane Potentials. *MRS Proc.* **2002**, *752*, AA8-11. [CrossRef]
18. Sokalski, T.; Lingelfelter, P.; Lewenstam, A. Numerical Solution of the Coupled Nernst-Planck and Poisson Equations for Liquid Junction and Ion Selective Membrane Potentials. *J. Phys. Chem. B* **2003**, *107*, 2443–2452. [CrossRef]
19. Lingenfelter, P.; Bedlechowicz-Sliwakowska, I.; Sokalski, T.; Maj-Zurawska, M.; Lewenstam, A. Time-Dependent Phenomena in the Potential Response of Ion-Selective Electrodes Treated by the Nernst-Planck-Poisson Model. 1. Intramembrane Processes and Selectivity. *Anal. Chem.* **2006**, *78*, 6783–6791. [CrossRef]
20. Sokalski, T.; Kucza, W.; Danielewski, M.; Lewenstam, A. Time-Dependent Phenomena in the Potential Response of Ion-Selective Electrodes Treated by the Nernst-Planck-Poisson Model. Part 2: Transmembrane Processes and Detection Limit. *Anal. Chem.* **2009**, *81*, 5016–5022. [CrossRef]
21. Vlasov, Y.; Legin, A.; Rudnitskaya, A.; Di Natale, C.; D'Amico, A. Nonspecific Sensor Arrays ("electronic Tongue") for Chemical Analysis of Liquids (IUPAC Technical Report). *Pure Appl. Chem.* **2005**, *77*, 1965–1983. [CrossRef]
22. Vlasov, Y.; Legin, A.; Rudnitskaya, A.; D'Amico, A.; Di Natale, C. "Electronic Tongue"—New Analytical Tool for Liquid Analysis on the Basis of Non-Specific Sensors and Methods of Pattern Recognition. *Sens. Actuators B Chem.* **2000**, *65*, 235–236. [CrossRef]
23. Hayashi, K.; Yamanaka, M.; Toko, K.; Yamafuji, K. Multichannel Taste Sensor Using Lipid Membranes. *Sens. Actuators B Chem.* **1990**, *2*, 205–213. [CrossRef]
24. Pereira, T.S.; Facure, M.H.M.; Mercante, L.A.; Gonçalves de Souza, M.H.; Braunger, M.L.; Riul, A., Jr.; Correa, D.S. Electronic Tongues: Basics, Materials, and Applications. In *Nature-Inspired Sensors*; Elsevier: Amsterdam, The Netherlands, 2025; pp. 451–465.
25. Vlasov, Y.; Legin, A.; Rudnitskaya, A. Electronic Tongues and Their Analytical Application. *Anal. Bioanal. Chem.* **2002**, *373*, 136–146. [CrossRef] [PubMed]

26. Ciosek, P.; Wróblewski, W. Potentiometric Electronic Tongues for Foodstuff and Biosample Recognition—An Overview. *Sensors* **2011**, *11*, 4688–4701. [CrossRef]
27. Tahara, Y.; Toko, K. Electronic Tongues—A Review. *IEEE Sens. J.* **2013**, *13*, 3001–3011. [CrossRef]
28. Vahdatiyekta, P.; Zniber, M.; Bobacka, J.; Huynh, T.-P. A Review on Conjugated Polymer-Based Electronic Tongues. *Anal. Chim. Acta* **2022**, *1221*, 340114. [CrossRef] [PubMed]
29. Vanaraj, R.; IP, B.; Mayakrishnan, G.; Kim, I.S.; Kim, S.-C. A Systematic Review of the Applications of Electronic Nose and Electronic Tongue in Food Quality Assessment and Safety. *Chemosensors* **2025**, *13*, 161. [CrossRef]
30. Rodrigues, D.R.; de Oliveira, D.S.; Pontes, M.J.; Lemos, S.G. Voltammetric e-tongue based on a single sensor and variable selection for the classification of teas. *Food Anal. Methods* **2018**, *11*, 1958–1968. [CrossRef]
31. Cortina, M.; Duran, A.; Alegret, S.; del Valle, M. A Sequential Injection Electronic Tongue Employing the Transient Response from Potentiometric Sensors for Anion Multidetermination. *Anal. Bioanal. Chem.* **2006**, *385*, 1186–1194. [CrossRef] [PubMed]
32. Legin, A.; Rudnitskaya, A.; Vlasov, Y. Electronic Tongues: New Analytical Perspective for Chemical Sensors. In *Comprehensive Analytical Chemistry XXXIX*; Alegret, S., Ed.; Elsevier Science: Amsterdam, The Netherlands, 2003; pp. 437–486.
33. Mimendia, A.; Gutiérrez, J.M.; Leija, L.; Hernández, P.R.; Favari, L.; Muñoz, R.; del Valle, M. A Review of the Use of the Potentiometric Electronic Tongue in the Monitoring of Environmental Systems. *Environ. Model. Softw.* **2010**, *25*, 1023–1030. [CrossRef]
34. Cuartero, M.; Ruiz, A.; Oliva, D.J.; Ortuño, J.A. Multianalyte Detection Using Potentiometric Ionophore-Based Ion-Selective Electrodes. *Sens. Actuators B Chem.* **2017**, *243*, 144–151. [CrossRef]
35. Bishop, C.M. *Pattern Recognition and Machine Learning*; Information Science and Statistics; Springer: New York, NY, USA, 2006; ISBN 978-0-387-31073-2.
36. Armstrong, R.D.; Horvai, G. Properties of PVC Based Membranes Used in Ion-Selective Electrodes. *Electrochim. Acta* **1990**, *35*, 1–7. [CrossRef]
37. Marcus, Y. Thermodynamics of Solvation of Ions. Part 5.—Gibbs Free Energy of Hydration at 298.15 K. *J. Chem. Soc. Faraday Trans.* **1991**, *87*, 2995–2999. [CrossRef]
38. Sakaki, T.; Harada, T.; Kawahara, Y.; Shinkai, S. On the Selection of the Optimal Plasticizer for Calix[n]Arene-Based Ion-Selective Electrodes: Possible Correlation between the Ion Selectivity and the 'Softness' of the Plasticizer. *J. Incl. Phenom. Mol. Recognit. Chem.* **1994**, *17*, 377–392. [CrossRef]
39. Rais, J.; Okada, T.; Alexová, J. Gibbs Energies of Transfer of Alkali Metal. Cations between Mutually Saturated Water-Solvent Systems Determined from Extraction Experiments with Radiotracer ^{137}Cs. *J. Phys. Chem. B* **2006**, *110*, 8432–8440. [CrossRef]
40. Osakai, T.; Ebina, K. Non-Bornian theory of the Gibbs energy of ion transfer between two immiscible liquids. *J. Phys. Chem. B* **1998**, *102*, 5691–5698. [CrossRef]
41. Yamashoji, Y.; Tanaka, M.; Nagamune, S.; Ouchi, M.; Hakushi, T.; Shono, T. Polymer Membrane Thallium(I)-Selective Electrodes Based on Dibenzo-Crown-6 Ethers. *Anal. Sci.* **1991**, *7*, 485–486. [CrossRef]
42. Mikhelson, K.N. Electrochemical Sensors Based on Ionophores: Current State, Trends, and Prospects. *Russ. J. Gen. Chem.* **2008**, *78*, 2445–2454. [CrossRef]
43. Mittal, S. PVC-Based Dicyclohexano-18-Crown-6 Sensor for La(III) Ions. *Talanta* **2004**, *62*, 801–805. [CrossRef] [PubMed]
44. Kikuchi, Y.; Sakamoto, Y. Complex formation of alkali metal ions with 18-crown-6 and its derivatives in 1, 2-dichloroethane. *Anal. Chim. Acta* **2000**, *403*, 325–332. [CrossRef]
45. Leon-Medina, J.X.; Anaya, M.; Tibaduiza, D.A. Yogurt Classification Using an Electronic Tongue System and Machine Learning Techniques. *Intell. Syst. Appl.* **2022**, *16*, 200143. [CrossRef]
46. Gabrieli, G.; Muszynski, M.; Thomas, E.; Labbe, D.; Ruch, P.W. Accelerated Estimation of Coffee Sensory Profiles Using an AI-Assisted Electronic Tongue. *Innov. Food Sci. Emerg. Technol.* **2022**, *82*, 103205. [CrossRef]
47. Gabrieli, G.; Muszynski, M.; Ruch, P.W. A Reconfigurable Integrated Electronic Tongue and Its Use in Accelerated Analysis of Juices and Wines. In Proceedings of the 2022 IEEE International Symposium on Olfaction and Electronic Nose (ISOEN), Aveiro, Portugal, 29 May 2022; pp. 1–3.
48. Archibald, R.; Gelb, A. Reducing the Effects of Noise in Image Reconstruction. *J. Sci. Comput.* **2002**, *17*, 167–180. [CrossRef]
49. Stanković, S.; Orović, I.; Stanković, L. An automated signal reconstruction method based on analysis of compressive sensed signals in noisy environment. *Signal Process.* **2014**, *104*, 43–50. [CrossRef]

Disclaimer/Publisher's Note: The statements, opinions and data contained in all publications are solely those of the individual author(s) and contributor(s) and not of MDPI and/or the editor(s). MDPI and/or the editor(s) disclaim responsibility for any injury to people or property resulting from any ideas, methods, instructions or products referred to in the content.